Prairie View A&M University AUV Robotics: Transitioning from the Panther to the PV Inspire

Cristina Luanga, Taiwo Akinola, Uzair Nadeem, Jason Ruth, Bridget Stewart, Scott Rossel, Johan Rhodes, Jasmine Stith, Christopher McLamb, Tariq Alam, Adama Kone, Renel Allen, Damon Alsup, Abideen Adegboyega, Morgan Anderson

***Abstract*— The Prairie View A&M Autonomous Underwater Vehicle (PV AUV) Robotics Team is an undergraduate team comprised of mechanical, electrical, and computer engineering students under the advisement of respective professors from within the Roy G. Perry College of Engineering. Innovations in autonomous subsea robots are extremely valuable to the oil and gas industry performing several underwater functionalities such as, but not limited to, mapping underwater terrain for potential oil reservoirs or monitoring and quickly fixing piping leaks. Through the exploitation and reimaging of existing technologies and methods utilized to manufacture current autonomous underwater vehicles (AUVs), the team designed, engineered, and programmed the *PV Inspire* to compete in the 2017 International RoboSub Competition.**

Entities that employ AUVs to do subsea work desire a robot that is intelligent and equipped to respond to a variety of underwater challenges quickly without any external assistance. Aiming to satisfy competition goals and provide solutions to industry matters, *the PV Inspire* is fashioned to exceed its predecessor *the Panther* in overall functionality, capable of interpreting and following visual cues, manipulating the environment, maintaining control under harsh underwater conditions, and executing desired tasks efficiently. The standard six thruster arrangement paired with an adjustable rod-clamp design ensures a high level of maneuverability and increases the vehicle's overall modularity. A downward facing camera allows the AUV to scope and follow the pool floor while a servo-operated, forward-facing camera aids in navigating the vehicle through its surroundings. The vehicle's navigational system, computational boards, and main power source are sealed within a large cylindrical hull, creating a simplistic, yet intricate and lightweight design.

I. Introduction

Established since 2011, PV AUV is a yearly senior design project structured to challenge a collaborative team of engineers of various disciplines to design and build a fully autonomous underwater vehicle, capable of competing in the AUVSI RoboSub Competition. This year students were originally tasked with redesigning, modifying, and enhancing Prairie View's longstanding AUV, *the Panther*. While the original design of the vehicle proved to be, in theory, structurally sound, the overall deterioration of the vehicle's frame, electrical connections, and unresolved water leakage inspired the PV AUV team to push the boundary and design a completely new sub. Hence, the *PV Inspire* was engineered not only to surpass its predecessor in the technical aspect, but to serve as a turning point for the engineering program at Prairie View, inspiring students to go beyond self-imposed limits and aspire to produce products of excellence.

II. Design Strategy

The *PV Inspire* is designed to satisfy four main project objectives: functionality, convenience, safety, and economic consideration. Restricted to primarily in-house fabrication, a limited budget, and a yearly time constraint, the team focused on creating a simple and effective, yet cost-efficient sub. A successful design that incorporates a high degree of modularity and maneuverability, target-tracking capabilities, sonar sensing, and a fully integrated navigational system hypothetically will allow the AUV to meet the basic navigational goals and leave room for future teams to develop the vehicle for additional task items.

In retrospect, previous teams designed a hull to fit a rigid frame and subsequently manipulated the weight and buoyancy according to the addition and placement of external housings. The open-frame design, for example, has a thin cross sectional frame for easy movement in the forward and backward directions. The selected material, Aluminum 6061, meets the demanding strength-to-weight ratio, possesses excellent resistance to corrosion, and is overall considered "good" [1] for underwater vehicle structures. In comparison to earlier variations of the AUV, the frame added a new level of modularity, allowing the thruster mounts to move freely from side to side along horizontal slots and adding additional screw holes for the mounts to be placed further up or down, vertically. However, the rigid structure configuration, which was designed to fit the hull in its entirety while remaining within the AUVSI maximum size constraints, limited the versatility for other, potential components and left little to no room for any major adjustments along the frame. Additional housings that accommodated components, such as the batteries and camera(s), added a level of modularity, but reduced the overall stability of the vehicle, causing unnecessary imbalances and buoyancy issues.

Focusing primarily on increasing modularity and reliability without sacrificing capability, this year's team opted to move most of the electronic and software components inside a single hull and design a frame capable of accommodating different shapes and thruster arrangements. The final design of the *PV Inspire*, shown in Fig. 1, utilizes simplified and easily accessible components

allowing for the adjustment of current parts and the retrofitting of any additional parts.

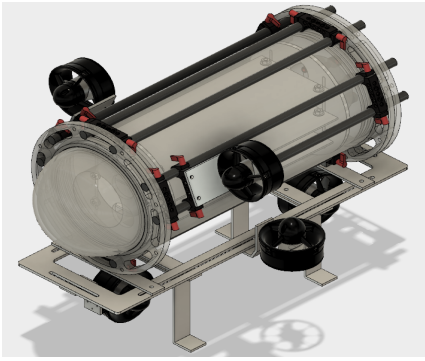

Fig. 1 Autodesk Fusion CAD rendering of the finalized *PV Inspire*

III. Vehicle Design

Initially, the design process was generated and outlined for the schedule, problem identification, project planning, and literature review phases. The team encountered a few technical problems with the literature review and was forced to reformat and clarify the content to demonstrate a solid understanding of AUV components and concepts. The extra time and effort allocated to the report extended the overall duration of the design process an extra four to five weeks past the expected completion date. However, using Microsoft Projects, the team collaboratively established an estimated timeline and Gantt Chart to meet the anticipated milestones and deliverables, as a well-planned and detailed schedule is key. While the team was unable to manufacture the components, assemble the AUV, or check the actual constraints of the finalized design as originally planned at the beginning of the semester, due to unavoidable circumstances, the Gantt Chart aided in monitoring the overall progression of the project, successfully serving as a guideline and checklist to help the team remain within the set timeframe.

A. Preliminary Design

By dissecting and grasping the failures and successes of previous design concepts applied to *the Panther*, the team acknowledged common mistakes and incorporated effective techniques and ideas into the current design. The preliminary design of the *Inspire* began with a functional decomposition flow chart that specified the main function the AUV needed to accomplish and sub-functions that explicitly define how the team would enable the vehicle to deliver. Given the difficulties experienced by previous teams in navigation and sensory tasks, the main function consisted of the AUV completing three specified competition tasks: passing through a validation gate, following a path marker, and navigating the channel gate. Enabling the vehicle to move to a specified destination and integrating the electronic components served as the two major sub-functions which shaped the ideas that populated the concept generation chart. Ideas were collectively evaluated and either denoted as a "GO" or a "NO-GO" based on general efficiency, effectiveness, and reliability. From there, ideas denoted as "GO" were discussed at length based on a more detailed set of criteria, considering additional factors such as how much time and funding the team would have to incorporate the concept, manufacturability, longevity, and whether the concept would keep the vehicle lightweight.

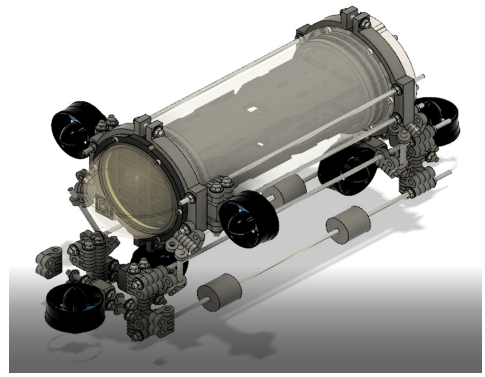

Fig. 2 Autodesk Fusion CAD rendering of the original *PV Inspire*

The modular design displayed in Fig.2 demonstrates the initial compilation of the resulting "GO" concepts and ideas from the decision-matrix selection process. This original design incorporated a minimum of fifty custom-made, adjustable hinges that connect to a series of threaded rods. A linear frame of almost any shape could be achieved using nuts and bolts to hold the rods in place, with the only access point into the hull located at the back of the AUV. While the custom hinge design increased the modularity, it reduced reliability and robustness, as each hinge represented an additional failure point and reduced the stability of the vehicle. Also, the hinges were not readily available and required customization, which posed another threat to the team's budget and project timeline. Therefore, the team's redesign of the *PV Inspire* (displayed in Fig. 1) maintains the same level of modularity while reducing the complexity in both the manufacturing and assembly of parts.

Table 1: The Overview of the *PV Inspire*

*The Weight listed in the table does not include the added weight needed to obtain neutral buoyancy as the vehicle is still being modified

Specification	Dimension (units)
Length	21.5 (inches)
Width	15.0 (inches)
Height	17.3 (inches)
Weight *	30.2 (inches)
Max Depth (Tested)	12 (feet)
Thrusters	6 x Blue Robotics T100
Camera(s)	2 x 8MP Raspberry Pi v2
Inertial Navigational System	1 x OpenROV Depth + Sensor
Operating Frameworks	Arduino IDE & Python

B. Mechanical Systems

Detailed process and design analysis equations and simulations were applied and conducted on all the AUV's major components. The gathered results further determined the reliability as well as the robustness of the vehicle and gave deeper insight to hidden failure points. Autodesk Fusion 360, ANSYS, and Siemens NX were all utilized to run analyses on various parts of the *Inspire*.

1) Cylindrical Hull

A cylindrical, acrylic hull, which serves as the main housing unit for all the electrical components (including the battery), is the only physical element being reused from *the Panther* [2]. Consequently, waterproofing plays a vital role in the design of the hull, being that if the seals around the hull fail, our vehicle will fail. A thorough hydrostatic analysis was simulated in Autodesk Fusion to ensure structure failure due to increased water pressure would not cause the hull to fail.

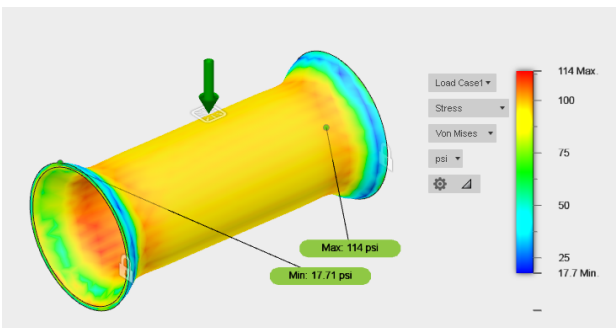

Fig. 3 Stress Analysis for the Hull

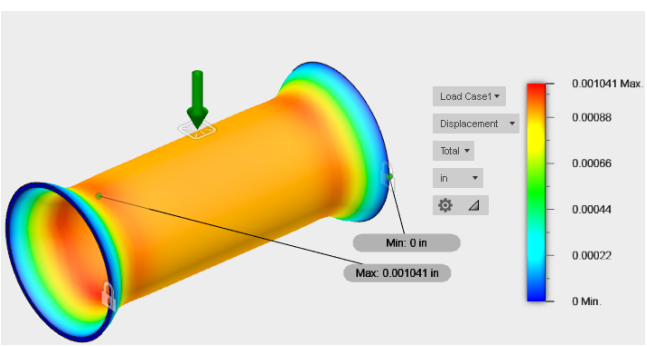

Figure 5.16 Displacement Analysis for Hull

At a competition depth of 16 feet, the pressure induced on the tube will be approximately 6.94 psi (pounds per square inch) as displayed in Fig. 3. Compared to the acrylic yield strength of 7092 psi, hull failure due increasing water pressure was determined to be ineffective. A deflection analysis was also conducted, resulting in a theoretical displacement of no more than .001 inches, which was determined to be insignificant in affecting the inner electronics as well as the surrounding external rods.

2) Hull Endcaps

The hull caps are an integral part of the hull sub-assembly, used to create a boundary between the aquatic competition environment and the electrical components housed within the hull's interior. Acrylic endcaps were constructed to seal the acrylic hull and hold the attached mounting rods which would serve as a surrounding frame. The custom-made aluminum endcaps used in the previous years performed adequately in sealing the electronic components. However, upon further investigation, the team realized that overly tight seal was due to incorrect an O-ring to groove measurement ratio. The heavy square-headed aluminum caps allowed previous teams to recklessly force the endcaps in and out of the hull with little to no consideration for accuracy or ease of removal. With no exact measurements or reliable O-ring selection process to reference from previous documentation, the mechanical team, due to a limited time constraint, was forced to manipulate the groove of the acrylic endcaps to properly fit the gasket. Fortunately, the team was given the opportunity to remake the endcaps and properly select O-rings using the compression and stretch recommendations, based on the following inner diameter and cross-sectional diameter equations [3].

$$ID = G_d(1 - S_{rec}) \qquad (1)$$

where,

- ID is the inner diameter of the O-ring
- S_{rec} is the bore diameter tolerance
- G_d is the groove diameter

$$CS_{max} = \left[\frac{(B_d - B_{tol}) - (G_d + G_{tol})}{2}\right]\left(\frac{1}{1 - C_{max}}\right) - CS_{tol} \qquad (2)$$

$$CS_{min} = \left[\frac{(B_d + B_{tol}) - (G_d - G_{tol})}{2}\right]\left(\frac{1}{1 - C_{max}}\right) + CS_{tol} \qquad (3)$$

where,

- CS_{max} is the maximum cross-sectional diameter of the O-ring,
- CS_{min} is the maximum cross-sectional diameter of the O-ring
- B_d is the bore diameter
- B_{tol} is the bore diameter tolerance
- G_d is the groove diameter
- G_{tol} is the groove diameter tolerance
- C_{max} is the maximum compression
- CS_{tol} is the cross-sectional tolerance

The stretch of the O-ring references how snuggly the seal fits into the groove, based on its circumferential stretch. A great seal will generally have a preferred stretch within 2% of its inner diameter value. Additionally, the O-ring will compress radially once it has settled in the gland. To meet the recommended maximum compression of 40%, the cross-sectional diameter of the O-ring must be greater than the overall effective depth of the groove.

The calculations for equations (1-3) were conducted in Engineering Equation Solver (EES) to theoretically determine the inner diameter and cross section of the O-ring needed to achieve an ideal seal compression against water. As a result, the following tables were generated, displaying all possible sizes, both standard and custom-made, that would provide the best seal for the acrylic endcaps. The tables displayed in Fig. 5-7, depict these results. The blue highlight indicates the base standard against which all other variations were compared. Purple indicates O-rings that failed the specified stretch and compression criteria. The yellow highlight represents results that were plausible but concerning. The manilla shade represents results that were still plausible but more likely to succeed due to certain exceptions. Finally, the green specifies results that were highly plausible and likely to properly seal the hull. To save time, all of the O-ring sizes that produced green results were purchased and manually tested for the best fit.

AS-568 Chart Comparison | ISO O-ring 3601 Chart Comparison | "Other O-ring sizes" -Apple Rubber Comparison

2.8	1 ID [in]	2 CS [in]	3 G_d [in]	4 S_{rec}	5 C [%]	6 GW [in]	7 OD
Run 1	7.526	0.1911	7.68	0.02	16.27	0.2867	8.062
Run 2	7.25	0.125	7.64	0.05105	-44	0.1875	7.89
Run 3	7.5	0.125	7.79	0.03723	16	0.1875	8.04
Run 4	7.25	0.1875	7.663	0.0539	10.13	0.2813	8.038
Run 5	7.5	0.1875	7.69	0.02471	17.33	0.2813	8.065
Run 6	7.75	0.1875	7.69	-0.007802	17.33	0.2813	8.065
Run 7	7.25	0.25	7.6	0.04605	20	0.375	8.1

Fig. 5 Side view of the Rear Acrylic Endcap

AS-568 Chart Comparison | **ISO O-ring 3601 Chart Comparison** | "Other O-ring sizes" -Apple Rubber Comparison

2.8	1 ID [in]	2 CS [in]	3 G_d [in]	4 S_{rec}	5 C [%]	6 GW [in]	7 OD
Run 1	7.526	0.1911	7.68	0.02	16.27	0.2867	8.062
Run 2	7.234	0.139	7.62	0.05068	-36.69	0.2085	7.898
Run 3	7.484	0.139	7.768	0.03658	16.55	0.2085	8.046
Run 4	7.734	0.139	7.768	0.004403	16.55	0.2085	8.046
Run 5	7.225	0.2098	7.6	0.04933	4.691	0.3148	8.02
Run 6	7.475	0.2098	7.65	0.02288	16.59	0.3147	8.07
Run 7	7.725	0.2098	7.72	-0.0006477	33.27	0.3147	8.14
Run 8	7.225	0.2751	7.55	0.04305	18.21	0.4127	8.1

Fig. 6 Side view of the Rear Acrylic Endcap

AS-568 Chart Comparison | ISO O-ring 3601 Chart Comparison | **"Other O-ring sizes" -Apple Rubber Comparison**

2..23	1 ID [in]	2 CS [in]	3 G_d [in]	4 S_{rec}	5 C [%]	6 GW [in]	7 OD
Run 1	7.526	0.1911	7.68	0.02	16.27	0.2867	8.062
Run 2	7.244	0.158	7.7	0.05922	5.063	0.237	8.016
Run 3	7.224	0.315	7.68	0.05938	49.21	0.4725	8.31
Run 4	7.283	0.177	7.68	0.05169	9.605	0.2655	8.034
Run 5	7.283	0.197	7.648	0.04772	10.66	0.2955	8.042
Run 6	7.283	0.209	7.644	0.04723	14.83	0.3135	8.062
Run 7	7.283	0.236	7.6	0.04171	15.25	0.354	8.072
Run 8	7.402	0.158	7.73	0.04243	14.56	0.237	8.046
Run 9	7.402	0.236	7.605	0.02669	16.31	0.354	8.077
Run 10	7.48	0.158	7.735	0.03297	16.14	0.237	8.051
Run 11	7.48	0.197	7.67	0.02477	16.24	0.2955	8.064
Run 12	7.48	0.209	7.65	0.02222	16.27	0.3135	8.068
Run 13	7.48	0.236	7.605	0.01644	16.31	0.354	8.077
Run 14	7.559	0.158	7.74	0.02339	17.72	0.237	8.056
Run 15	7.581	0.215	7.65	0.00902	18.6	0.3225	8.08
Run 16	7.61	0.158	7.738	0.01654	17.09	0.237	8.054
Run 17	7.618	0.197	7.69	0.009363	21.32	0.2955	8.084
Run 18	7.638	0.118	7.78	0.01825	6.78	0.177	8.016
Run 19	7.638	0.224	7.64	0.0002618	19.64	0.336	8.088
Run 20	7.677	0.118	7.805	0.0164	17.37	0.177	8.041
Run 21	7.677	0.158	7.75	0.009419	20.89	0.237	8.066
Run 22	7.677	0.236	7.61	-0.008804	17.37	0.354	8.082
Run 23	7.734	0.139	7.77	0.004633	17.27	0.2085	8.048

Fig. 7 Side view of the Rear Acrylic Endcap

The endcaps were manufactured, layer-by-layer, using a Model 10000 Epilog Zing Laser. Each layer circle was drafted in AutoCAD, accounting for every penetrator, connector, or slot hole, and then acrylic cemented one to another, as displayed in Fig. 8.

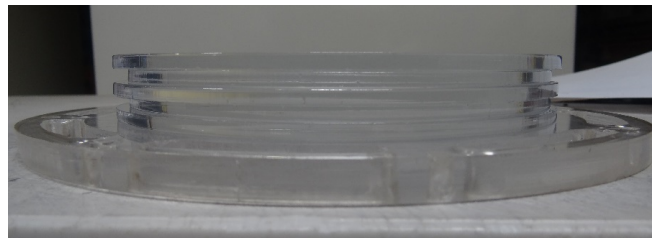

Fig. 8 Side view of the Rear Acrylic Endcap

The team mistakenly purchased acrylic adhesive instead of acrylic cement which caused water to leak in between each layer of the endcap. Subsequently, during the remake of the endcaps, that mistake was taken into consideration and corrected, which partially contributed to the resolve of waterproofing problem.

A stress analysis was conducted to determine probable failure under 60lbf (pound force) of reactionary force – the result of an extreme weight scenario of the summed AUV weights and components needed to counteract excessive buoyancy. The forces applied to the analysis were originally specified to be the reaction forces from the stress caused by the weight of the AUV, while lifted, with the minimum force that would be required to carry the AUV into water. Both the stress and deflection were minimal and most likely would not cause the geometries to fail, as the results were far beneath the maximum yield strength. The results of the stress and displacement are displayed in Fig. 9 and Fig. 10 respectively.

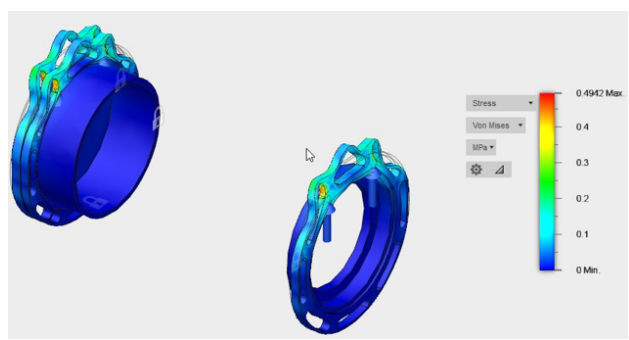

Fig. 9 Stress Analysis of the Front and Back Endcaps

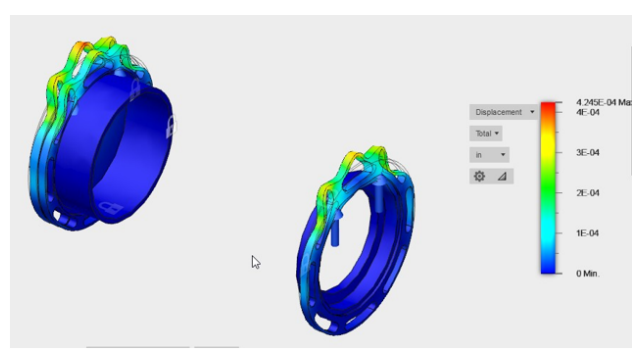

Fig. 10 Displacement Analysis of the Front and Back Endcaps

The acrylic dome, which is acrylic cemented to the front endcap, houses the camera enabling the AUV to have a comprehensive and transparent viewing window. This will allow *the Inspire* to visually interpret the surrounding environment and adjust itself accordingly.

Apart from vision sensory, the dome also serves the purpose of ensuring that vehicle maintains a laminar shape. In Fig. 11, a streamline velocity analysis was conducted through ANSYS to simulate the moving velocity of the AUV through a fluid, or relatively speaking a body of water. Based on the results, the overall geometry of the vehicle does not alter the laminar flow of the vehicle, making it easier for the AUV to maneuver.

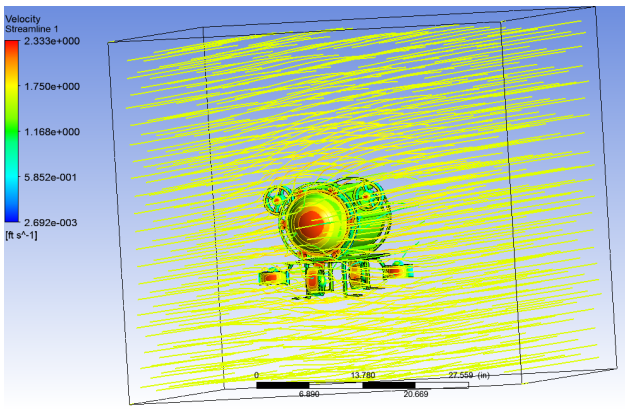

Fig. 11 ANSYS rendering of a Streamline Velocity Analysis (Front View)

3) Thrusters

The Blue Robotics T100 thrusters supply the necessary force to propel the vehicle and allow it to navigate in a desired direction (forward, backward, left, right, up, down). The design of *the PV Inspire* allows each of the six thrusters to be moved to relatively any position along its respective axis (Fig. 12).

Fig. 12 Example of Thruster Modularity Along Platform Base

A hydrostatic pressure contour was conducted to determine the best positioning for the thrusters. The side-thruster configuration displayed in Fig. 13, allows for the best equal distribution of the pressure along the front of the vehicle, rather than in one area. Although the positioning of the side-thrusters appears to perform best at a higher altitude, keeping them aligned with the center of pressure will always yield favorable results.

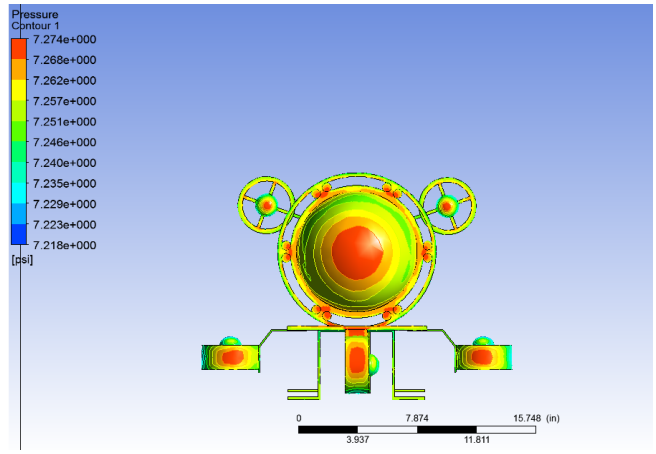

Fig. 13 ANSYS rendering of a Pressure Contour Analysis (Front View)

4) Electronics Rack System

In retrospect, gaining access to electronics within the hull has always been inefficient and ineffective. Generally, once the primary housing unit was removed from the frame, one of the aluminum endcaps served as a foot platform, while the other cap was pried from the opposite end. However, the acrylic material is significantly weaker in comparison to the aluminum, and cannot withstand the same tensile stresses. In addition to correcting the endcap groove diameter to properly fit the O-ring, this year's team implemented a quick release design, using cam levers to easily compress and decompress the inner gasket seal.

The physical framework of the actual tray has transformed over the course of the year to accommodate the varying electrical system designs. Originally, a series of three high density polyethylene (HDPE) trays were mounted, to two circular end chassis, one on each side, using L-brackets, nuts, and bolts to adjust the positioning anywhere along the z-axis. As shown in Fig. 14, this design was developed to hold two 16000mAh (milli-Ampere hours) and one 20000mAh Lithium Ion batteries, as well as two additional pounds of electronic components.

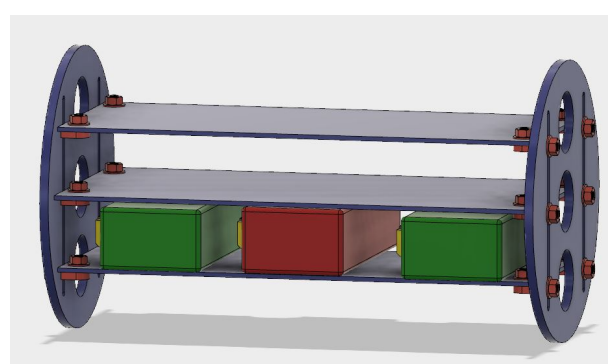

Fig. 14 Autodesk Fusion CAD rendering of original electronics rack

The assembled tray was secured in an upright position using a series of 1" standoffs connected from a triangular set of pre-threaded holes on the back chassis to pre-threaded holes in the rear endcap. The idea was for the electronic tray to be immediately accessible once the rear endcap was removed.

Unfortunately, the electrical system that the collaborative team originally designed for, was unable to be completed. Consequently, a new electronics rack was redesigned and tailored to fit a new electrical system. Different from the previous design, the current framework consists of two, durable, Delrin racks that horizontally slot into the end chassis on each side. Custom-fit bolts also screw horizontally through the pre-determined holes to hold the full assembly together. The length of the rack was also expanded to occupy more of the hull space and accommodate more components if necessary. Each part of the electronics rack system was also machined using a Model 10000 Epilog Zing Laser.

5) Frame Rods

The aluminum camera rods appended to the sides of the hull will serve as a pseudo-frame for mounting the thrusters, adding dead weight, and attaching other various components deemed necessary upon testing, presently and in the future. Each full length 15mm black aluminum alloy rod is a compilation of one 16-inch and one 4-inch rod, threaded together to achieve a total length of 20-inches. Alternatively, one 16-inch rod paired with one 6-inch, 15mm rod may be used to achieve a total length of 22 inches, if deemed necessary. Each rod is positioned around the hull, using the pre-defined slots around the endcaps for alignment. The rod clamps aid in this endeavor, securing the rods in place to prevent sliding.

A stress analysis for the Aluminum 6061 hollow rods was conducted with the attached rod clamps to determine loaded vertical stress and to simulate the stress of the mounted components, such as the thrusters and any additional components that may need to be mounted. The loaded force was tested at 25lbf, which includes the weight force of the thrusters, propulsion, and possible added weights to counteract buoyancy.

The stress was determined to be under 10 kpsi, which is within the range of 3000-8000 psi based on Fig. 15, with the stress concentrated in the center of the rod length based. Even the maximum stressed incurred stayed below the maximum yield of 40kpsi, and caused minimal deflection, as displayed in Fig. 16, with a maximum displacement of .041 inches.

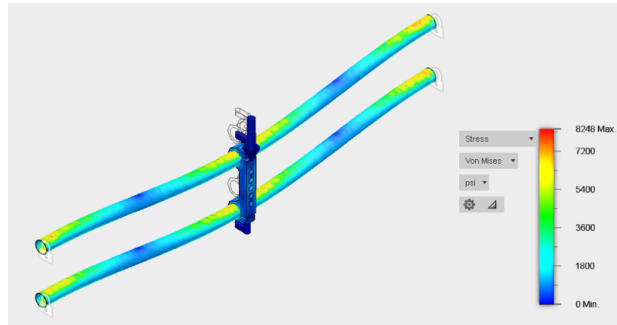

Fig. 15 Von Misses Stress Analysis of Camera Rods with Rod Clamp

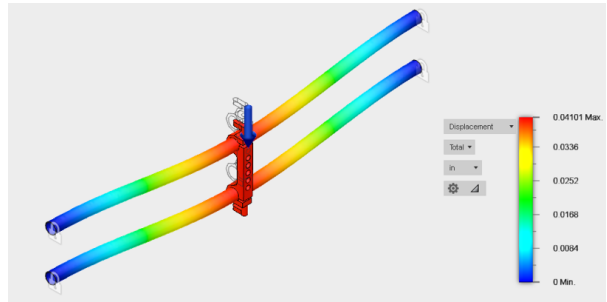

Fig. 16 Displacement Analysis of Camera Rods with Rod Clamp

6) Aluminum Platform Assembly

A computer numerical control (CNC) machine was used to manufacture an aluminum 6061 plate into a mounting platform. The frame from previous years served as a protective barrier around the hull as well as a base for additional components and dead weight to be mounted. With the removal of the rigid frame, added components could only be attached to the aluminum rods surrounding the hull. The original functionality of the platform was to serve as a foundation for the four ground thrusters, two up and down and two side to side.

Fusion 360 was used to find the total buoyant force and the center of buoyancy (CB). As shown in Fig. 17, the assembly is "joined" as a solid piece with uniform density.

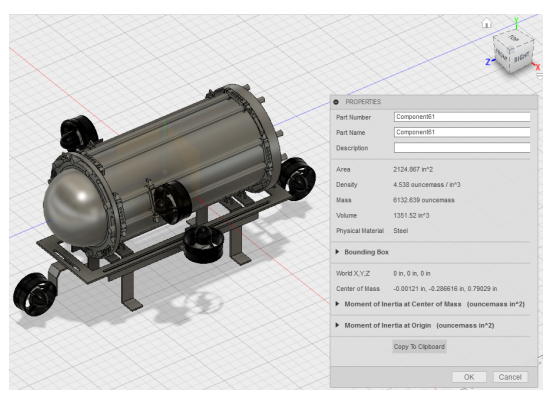

Fig. 17 Autodesk Fusion Rendering of Center of Buoyancy Calculations

For this new piece, the center of mass (CM) function was now able to find the CB of the original piece. The

"Properties" function was then used to show the total volume and CB:

CB (with respect to the origin): {-0.00121 in, -0.286616 in, 0.79029 in}

Volume: 1351.52 in^3

Given the total volume (V) and estimated specific volume of sea water (w), buoyancy (B) can be determined using the relationship [4]:

$$B = Vw \qquad (4)$$

where,

B is the buoyant force,
V is the volume of the displaced fluid, and
w is the specific weight of the fluid (sea water in this case).

Given,

$V = 1351.52\ in^3$
$w = 64\ \frac{lbs}{ft^3}$,

The buoyant force (4) was computed to be 50.56lbs.

The total mass and CM were also calculated using Fusion 360. After the correct individual masses and positions were set, the total mass was found to be roughly 30.4lbs. The "Center of Mass" function was then used, as shown in Fig. 18, and found, directly below the center of buoyancy, indicated by a blue circle (CM) and then a white circle respectively (CB).

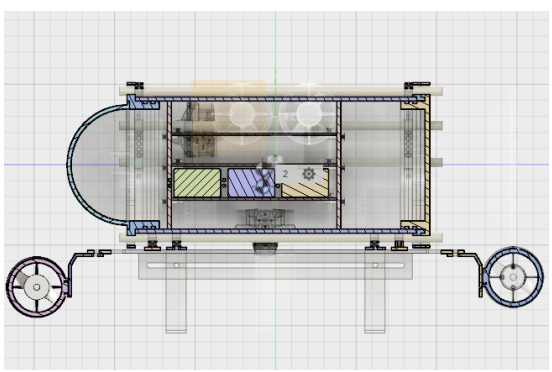

Fig. 18 Autodesk Fusion Rendering of CM and CB Coordinate Results

Additionally, based on the values shown in Table 2, while both the 'x' and 'z' values are roughly the same, the CM is nearly one inch lower than the CB. A visual representation of the results is also incorporated and displayed in Fig. 18.

Table 2: Coordinate Results for the CM and CB

Specification	x	y	z
Center of Mass	-0.008 in	-1.377 in	0.753 in
Center of Buoyancy	-0.001 in	-0.288 in	0.790 in

Because the center of mass is directly below the center of buoyancy, the AUV will be statically stable in rotation. However, since the buoyancy is over 20lbs higher than the weight, it will not be statically stable in the 'up-down' direction.

Realizing that the need to counteract the vehicle's natural buoyancy and achieve a state of neutrality would require a significant amount of dead weight, the platform was redesigned to accommodate more elements [4].

Aluminum 6061 was tested for the AUV leg support and loaded with 60lbf, accounting for any extra weight beyond the estimated 50lbs necessary for the AUV to counteract buoyancy. The load for one leg is exaggerated, even though the load is shared between two, to observe the effects of stress based on material and geometry. The test confirms that under a severe weight bearing, the legs possess the capability to withstand great stress tolerances beyond the estimated total weight of the AUV. The stresses in the analysis falls below the maximum yield point, which is 40 kpsi. The deflection analysis also indicated that even at the point of maximum deflection, the stress is far from the maximum yield point. Even though the legs were manufactured, by first heating the metal with a blow torch and then manually bending the piece in a bending machine at pre-measured points, the respective analyses displayed in Fig. 19 and 20, held true.

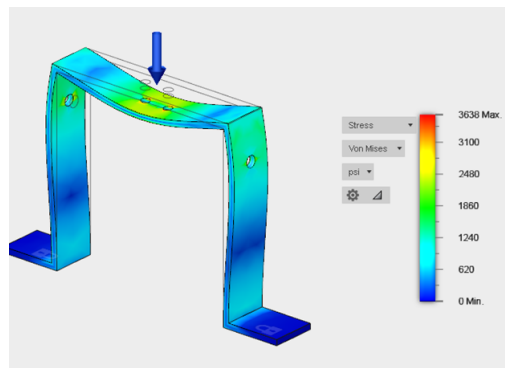

Fig. 19 Autodesk Fusion Rendering of CM and CB Coordinate Results

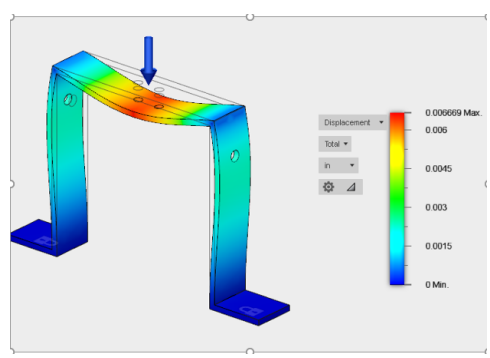

Fig. 20 Autodesk Fusion Rendering of CM and CB Coordinate Results

7) *Mounting Brackets*

The mounting brackets serve as a medium to attach the thrusters to the AUV. Each bracket is tailored to fit any thruster and can be moved in relatively any direction or

relocated anywhere on the sub. There are two main types of brackets, the thruster plates (Fig. 21), which are designed to accommodate the side thrusters and the modified L-shaped mounting brackets (Fig. 22), which are designed to accommodate the four thrusters attached to the aluminum platform.

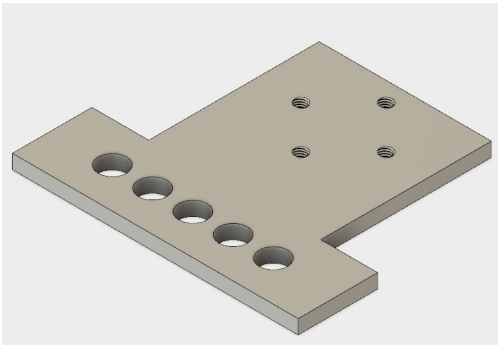

Fig. 21 Autodesk Fusion Rendering of Thruster Plates

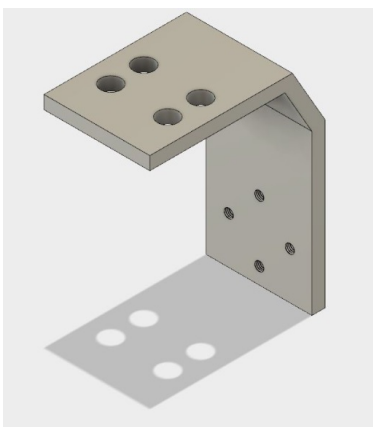

Fig. 22 Autodesk Fusion Rendering of Modified L-brackets for Thrusters

C. Electrical Systems

The greatest lesson the team learned in the development and integration of the electrical system was contingency. Given the experiences of the teams in previous years, navigation and system control has continually been a problem for the PV AUV team. This year, however, the original plan for the electrical system completely failed and was unable to be completed in time for testing. As with any engineering project, each member of the group is assigned a task or part that contributes to the final product. However, if any member of the team is unable to deliver, the final product must still be completed by the project deadline. Hence, the development of a second electrical system began in late March and was completed by mid-April. The second system was designed to complete the basic functionalities needed to carry out the aforementioned, navigational tasks, leaving room for expansion building towards the competition and future endeavors. The current layout of the electrical systems, displayed in Fig. 23 and Fig. 24, is still currently being developed and tested in preparation for the competition in July.

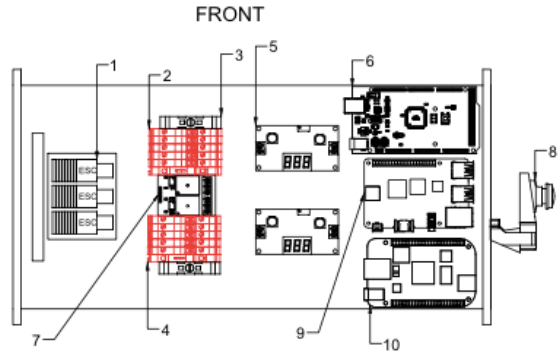

Fig. 23 AutoCAD 2D drawing of the modified electronics tray (top/front view)

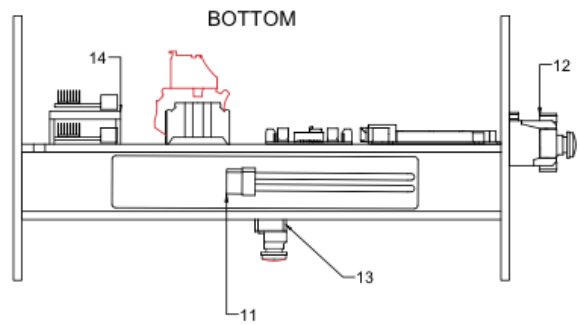

Fig. 24 AutoCAD 2D drawing of the modified electronics tray (side view)

1) Power System

The *PV Inspire* is powered by a single 14.8V, 20Ah Li-Po battery, located on the second tray of the electronics control system rack (ECSR) shown in Fig. 24 (11). The battery's capacity is sufficient to provide run time of at least two hours of which far exceeds the fifteen-minute time limits for actual and practice run segments of the competition.

The power supplied by the battery is conditioned by way of two solid-state relays (SSR), when individually switch enabled, distributes power through 2 branches within the electronic control system rack (ECSR). Switch one sources power through SSR-1, through to a LM2596 Buck Step-down DC voltage regulator which conditions the voltage to the recommended input operating parameters for the microcontroller boards. Switch two sources power through SSR-2, directly to a twelve-gang terminal block (TB-1), wired to individually power each of the electronic speed controllers (ESC) that operate its associated connected thruster. Uniquely assigned (addressed) output pins on the Arduino microcontroller is wire to each ESC, providing enabling control signals to the thrusters. The camera(s) are operated and controlled from the BeagleBone Black microcontroller board.

2) Computer & Software System

Currently, each functional component of *the PV Inspire* is operated by one of three microcontrollers: the Arduino

Mega 2560 Rev3, the BeagleBone Black, or the Raspberry Pi 3 Model B. Originally, each board was responsible for one major component or functionality of the *Inspire*. However, based on limited time and complexity of the programming, most if not all functionalities will be run using the BeagleBone Black. This will also include the camera which was originally selected to work with the Raspberry Pi board.

IV. Experimental Results

Primary testing was directed to thoroughly waterproofing the hull as the aforementioned problems with the acrylic endcaps made this task impossible. After the remake of the endcaps and a change in lubrication, petroleum jelly to silicon grease, waterproofing was no longer an issue and allowed for the integration and implementation of the electronics. As shown in Fig. 23, the *Inspire* was initially tested with linear coding, run directly from the Arduino IDE platform and operated by an Arduino Uno Microcontroller.

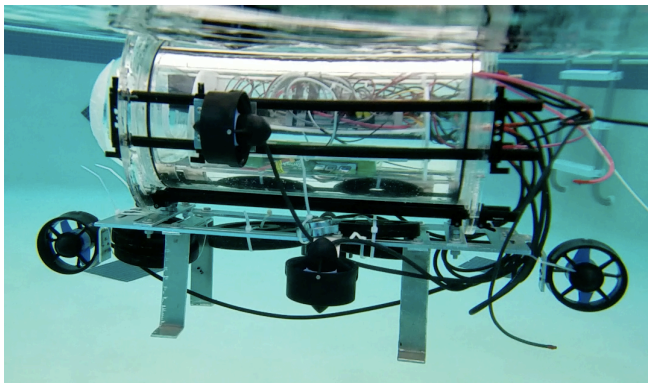

Fig. 23 Underwater shot of the *PV Inspire* during testing

During this phase of testing, the team observed and confirmed that while the AUV maintained balance and was statically and dynamically stable, there is not enough dead weight to keep the vehicle neutrally buoyant. Currently, certain components of the vehicle are being modified to help reduce buoyancy and add weight.

The new electrical rack system is almost complete and will be implemented within a week or two. Although the thruster configuration has been completed, the programming for the camera processing, as well as the IMU and depth sensor is still being calibrated. Additional functionalities of the *PV Inspire* will be incorporated based on time. In the future, testing of the electronic components should begin during the first semester to minimize unforeseeable mishaps such defective or unnecessary parts. Extra consideration to minor details as well as improved accountability from individual teams, mechanical, electrical and computer engineering, will allow the collaborative team to arrange more testing time and less contingency options.

V. Acknowledgements

The Autonomous Underwater Vehicle Senior Design Team (PV AUV) would like to thank Naval Sea Systems Command (NAVSEA) for their continued technical support and sponsorship.

We would also like to acknowledge Dr. Xiaobo Peng and Dr. Paul O. Biney for providing us with valuable feedback and advice throughout the duration of this challenging project. Additionally, we would like to thank industry professionals Mr. Homer Stewart, Werner Sopon (Panelmatic Texas Inc.), and Ali Rizvi for their time, dedication and expertise provided for the completion of the AUV; without them, this project would not be possible. We also thank the electrical engineering department and students for their efforts in this project. Last, we would like to thank the student Christian Smith for his support during manufacturing of the AUV.

VI. References

[1] Moore, Steven W., Harry Bohm, and Vickie Jensen. Underwater Robotics: Science, Design & Fabrication. Monterey, CA: Marine Advanced Technology Education Center, 2010. Ch. 4. pp.157-202

[2] Moore, Steven W., Harry Bohm, and Vickie Jensen. Underwater Robotics: Science, Design & Fabrication. Monterey, CA: Marine Advanced Technology Education Center, 2010. Ch.5. pp. 203-205

[3] "Design Guideline for Radial Seals." *Engineering Fundamentals.* EFunda Inc., 2017. Web. 02 July 2017.

[4] Moore, Steven W., Harry Bohm, and Vickie Jensen. Underwater Robotics: Science, Design & Fabrication. Monterey, CA: Marine Advanced Technology Education Center, 2010. Ch. 6. pp. 247-250